Light Metals — From ***Light Metals 1983***, E.M. Adkins, Editor

STRUCTURAL CHANGES IN CARBON BY HEAT TREATMENT

S.R. Brandtzæg[1,2], H. Linga[2], H.A. Øye[1]

[1] Institutt for uorganisk kjemi
Norges tekniske høgskole
Universitetet i Trondheim
N-7034 Trondheim-NTH, Norway

[2] Årdal og Sunndal Verk a.s.
N-5875 Årdalstangen, Norway

Anthracite has been calcined under controlled conditions. Weight loss, impurity content, pore volume, specific density, mean crystallite height, interlayer spacing and specific electrical resistivity have been measured at varying heating rates, temperatures and holding times. A model has been developed which expresses the electrical conductivity as a function of temperature and holding time. The model is used to estimate the mean electrical conductivity of calcined anthracite when the temperature gradient in the electrical calciner is assumed to be linear.

1. Introduction

Anthracite is the main raw material for cell linings in the Hall-Heroult process. Prior to use, anthracite is calcined in electrical furnaces or by gas firing.

Anthracite calcined in a gas fired rotary kiln is usually heat treated at temperatures around 1150°C. Graphite or coke is often added to gas calcined anthracite in order to increase the electrical conductivity. Average heat treatment temperature during electrical calcination is between 1750 and 1900°C. The temperature profile may vary from about 1200°C at the wall of the calciner to 2500°C near the electric arc.

In this work, we focus on structural changes in anthracite which are induced by heat treatment over a wider temperature range than usual (1,2). A detailed study of the change in electrical resistivity is also presented.

The following properties of the anthracite were analysed before and after heat treatment:

i) Ash content

ii) Impurity content of: Fe, Mn, S, Si and Ti

iii) Pore volume

iv) Specific density

v) Crystallographic properties
   a) Interlayer spacing, d_{002}
   b) Crystallite height, L_c

vi) Specific electrical resistance.

Thermogravimetric measurements were also carried out at the same temperatures and under identical experimental conditions as the heat treatment.

2. Experimental

Material

Commercially available german anthracite with particle size 4.0-5.6 cm was used as raw material.

Apparatus

Two different types of furnaces were used to cover the temperature range up to 2400°C. A water cooled Kanthal wound vertical laboratory furnace was used up to 1000°C with atmospheric pressure of nitrogen. The heating rate was automatically controlled. A graphite tube furnace was used to achieve temperatures above 1000°C. Argon at a pressure of 300 torr was used as inert gas. The temperature was measured by means of an optical pyrometer, and the heating rate was controlled by a linear effect controller. Below 760°C the temperature could not be measured by the optical pyrometer. This caused a nonlinear heating rate at lower temperatures. Temperature measurements with the optical pyrometer were often rendered inaccurate by clouding of the sight port. However, we were able to correct for this and the temperatures are considered reliable to ±10°C.

Basically identical furnaces to those described above were used for thermogravimetric measurements. The atmosphere and pressure were as described

above. The balances were of the knife edge type with an accuracy of 0.002 grams. The weight loss was continuously recorded.

Standard apparatus and methods were used for ash analysis. The X-ray measurements were carried out in a standard diffractometer. Ni-filtered Cu-radiation was used.

A Carlo Erba mod. 200 mercury porosimeter was used to determine pore volume and specific density in heat treated anthracite. The pressure was varied up to 1400 kg/cm^2 which corresponds to pores with radii between 54 and 75000 Å.

Procedure

Anthracite samples (40 grams) were heat-treated at different temperatures in the region 400-2400°C. The heating rate at temperatures below 1000°C was 400°C/h. At higher temperatures the heating rate was 200°C/h or 400°C/h. The holding time at maximum temperature was varied between 3 and 6 hours.

About 8 grams of the sample was heated in oxidizing atmosphere and held at 1000°C for 3 hours to determine the ash content.

About 5 grams of the sample was used for the pore analysis. The mercury penetration in the anthracite was continuously monitored as a function of pressure. A detailed procedure is described by Ritter and Drake (3), and Neher (4).

The content of Fe, Mn, S, Si and Ti was measured by X-ray fluorescense and the interlayer distance by X-ray diffraction. The crystallite height was calculated by using the half width of the 002-reflection. This method is described by Ergun (5).

Electrical resistivities of heat treated anthracite were determined by the voltage drop when a current of 1A was sent through a grinded sample (40-65 mesh) which was pressed between two electrodes in an insulated cylinder. The diameter of the cylinder was 25 mm, and the sample height was set to be 25.5 mm at a pressure of 42.5 kg/cm^2. The dependence on the sample height, the sample diameter and the isostatic pressure was also studied.

Thermogravimetric measurements were carried out under identical conditions as the heat treatments. The holding time at 600, 800, 1000, 1200, 2000 and 2400°C was 6 hours. The heating rates to maximum temperatures below 1000°C were 30°C/h or 360°C/h. The heating rates to maximum temperatures above 1000°C were 200°C/h or 400°C/h.

Structural Changes of Anthracite by Heat Treatment

Weight loss

Figure 1 shows the weight loss of anthracite *versus* temperature at different heating rates. At 600, 800, 1000, 1200, 1600, 2000 and 2400°C the isothermal weight loss attained after additional holding times of 1 and 6 hours also are shown. Due to lack of optical pyrometric temperature measurements, weight loss curves are not shown below 1000°C for samples which were heated above this temperature. Because different heating rates were used below 1000°C the weight loss curves are non-continuous at this temperature.

Fushizaki *et al.* (6) suggest that up to 200°C, weight loss results from drying of the coal. It was found that the weight loss levelled off at 150-200°C, as can be seen from Figure 1. Moisture content determined from weight loss up to 200°C was 1.3%. The figure shows that the weight loss increases from 350-400°C and levels off near 1000°C. Maximum weight loss rate occurs around 600-700°C. In this region the weight loss is due to volatilization of different hydrocarbons (7). At higher temperatures the weight loss rate increases until 1600°C where the rate again levels off. The total weight loss at 2400°C is 11.3%.

Figure 2 shows a parallel decrease of the S, Si, Fe and Mn content in the region from 1600°C to 2400°C. The content of Ti was constant at all temperatures up to 2400°C.

Generally, the influence of the heating rate on the weight loss is lower at higher temperatures. At 1000°C the difference in weight loss at heating rates of 30°C/h and 360°C/h is 0.8%. At 2400°C, the difference between weight loss at heating rates of 200°C/h and 400°C/h is negligible.

The isothermal weight loss during the first hour of holding time is about the half of the total isothermal weight loss after 6 hours.

Pore analysis

The pore volume of heat treated anthracite is shown in Figure 3a. In untreated anthracite the porevolume is 0.028 cm^3/g. After heat treatment at 400°C for 4 and 6 hours the pore volume is increased to 0.033 cm^3/g and 0.040 cm^3/g, respectively. Further heat treatment up to 1000°C causes a reduction in the pore volume to 0.027 cm^3/g. At higher temperatures the pore volume increases, and at 2400°C it is 0.10 cm^3/g. The influence of holding time decreases with increasing temperature.

The cumulative pore volume is shown in Figure 4. The figure shows that anthracite heat treated at temperatures below 1000°C have a pore radius less than 1000 Å. At higher heat treatment temperatures, about 50% of the pore volume is caused by pores with radius greater than 1000 Å.

The decreasing pore volume in the temperature region from 400°C to 1000°C is a result of a shrinkage process. In agreement with Miura and Silveston (8), we find that this process take place in the region 600-1000°C. The increasing pore volume in anthracite which has been heat treated to higher temperatures is a result of formation of new pores and pore growth through gas evolution. The simultaneous increase in density in this temperature region shows that the fraction of closed pores decreases.

Specific density

Figure 3b shows the specific density of heat treated anthracite. Anthracite heat treated to 400°C for 6 hours have lower specific density than the sample heated at 400°C for 4 hours, and even lower density than the untreated material. From 600°C the density increases with increasing heat treatment temperature up to 1200°C. From 1200°C to 1600°C the specific density decreases slightly and from 1600°C to 2400°C the specific density increases from 1.75 cm^3/g to 1.90 cm^3/g.

Expansion of closed pores is probably responsible for the low density in the samples heated at 400°C. As discussed above the shrinkage prosess is responsible for the decreasing pore volume in the temperature region 600-1000°C. The shrinkage process also leads to higher density. The release of sulphur

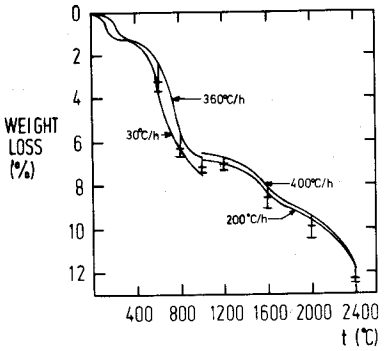

Figure 1. Weight loss (%) *versus* heat treatment temperature (°C) at different heating rates. Weight loss after isothermal treatment in 1 and 6 hours is indicated at 600, 800, 1000, 1200, 1600, 2000 and 2400°C.

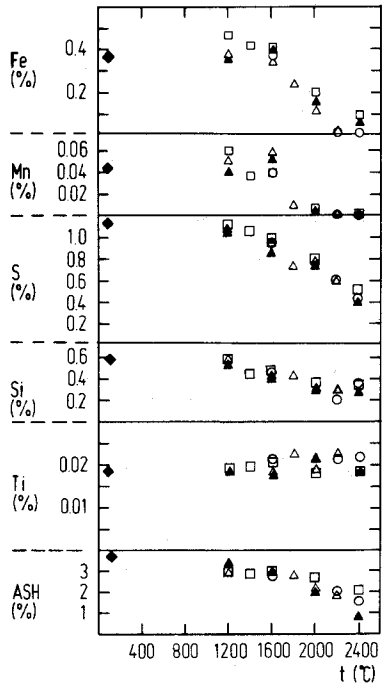

Figure 2. Impurity content (weight%) *versus* heat treatment temperature at different heating rates and holding times. (□ - 400°C/h, 3h; o - 400°C/h, 4h; Δ - 400°C/h, 6h; ▲ - 200°C/h, 6h). The impurity content in untreated anthracite is also shown (◆).

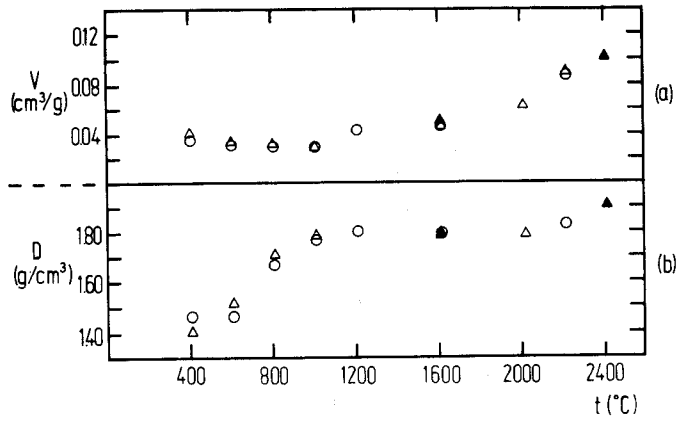

Figure 3. Pore volume (V) and spesific density (D) of anthracite *versus* heat treatment temperature at different heating rates and holding times. (□ - 400°C/h, 3h; o - 400°C/h, 4h; Δ - 400°C/h, 6h; ▲ - 200°C/h, 6h).

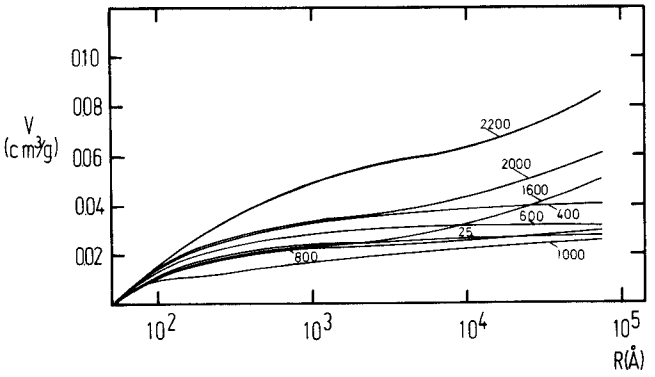

Figure 4. Cumulative pore volume of heat treated anthracite *versus* pore radius at different heat treatment temperatures (°C). The heating rate and holding time were 400°C/h and 6 hours, respectively.

which usually occurs at temperatures higher than 1500°C (Fig. 2), causes appreciable irreversible bulk expansion effects and leads to lower density (9, 10, 11).

X-ray measurements

The increase in density of the anthracite heat treated in the region 1800-2400°C is accompanied by a decrease in interlayer spacing and increase in crystallite height, see Figure 5. The crystallographic parameters of the anthracite samples heat treated to temperatures lower than 1800°C are not given due to a too weak signal for the d_{002} reflection.

The interlayer spacing decreases continuously with increasing heat treatment temperature from 1800°C to 2400°C where the values are 3.40 Å and 3.359 Å, respectively. The crystallite height increases from 52 Å to 139 Å in this region.

The influence of heating rate and holding time on the crystallographic parameters are relatively small compared with the maximum temperature.

The degree of graphitization, g, see Figure 5, is calculated from the values of interlayer spacing, d_{002}, and the equation of Maire and Mering (12)

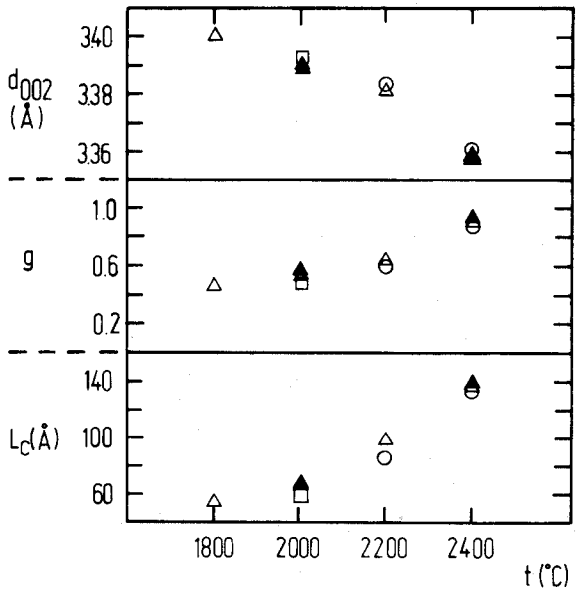

Figure 5. Interlayer spacing d_{002}; degree of graphitization, g, and crystallite height, L_c, of anthracite *versus* heat treatment temperature at different heating rates and holding times. (□ - 400°C/h, 3h; o - 400°C/h, 4h; Δ - 400°C/h, 6h; ▲ - 200°C/h, 6h).

$$g = (3.44 - d_{002})/0.086 \quad (1)$$

where:

3.44 - interlayer spacing (Å) in amorphous carbon

d_{002} - interlayer spacing in heat treated carbon.

The degree of graphitization varies from 0.47 at 1800°C to 0.92 at 2400°C. The change in interlayer spacing and the degree of graphitization, which is 0.92 at 2400°C, will be small at higher temperatures. At these temperatures the crystallite height will be a better indicator of the graphitization process.

The properties of anthracite, as for all carbonaceous materials, are affected to a considerable degree by the ash impurity content which is present in the initial anthracite. Graphite formation in heat treated anthracite coal, as revealed by X-ray measurements is promoted at relatively low temperature. Evans, Jenkins and Thomas (13) claim that the presence of impurity particles acts as catalytic sites for graphitization. The results from ash analysis show that the impurity content varies from about 3% to approximately 1.5% in the region where the graphitization process proceed.

Electrical resistivity

Determination of the electrical resistivity in powdered anthracite shows that for identical samples, small variations of the measuring procedure leads to distinctly different results. Figure 6 shows the effect of the isostatic sample pressure, the sample height and the sample diameter.

The sample pressure determines the contact area and number of contact points between the grains. Thus high pressures leads to lower resistivities. The relative influence of interface effects between the electrodes and the isolated cylinder wall of the sample holder and the grains in the sample, decrease with increasing sample size, and cause lower resistivities in larger samples.

Figure 7 shows the electrical resistivity in heat treated anthracite. The experiments were carried out under identical conditions. The sample height was kept at 25.5 mm, the sample diameter was 25.0 mm and the isostatic pressure was 42.5 kg/cm^2.

The electrical resistivity in untreated anthracite is infinite. In anthracite heat treated to 1200°C the resistivity measured by this method is reduced to 0.079 ohm cm and it is further reduced to 0.027 ohm cm at 2400°C.

Increasing holding time causes lower electrical resistivity, but the effect is small and decreases at higher temperatures.

4. Estimation of Electrical Resistivity in Heat Treated Anthracite

Richards (14) studied crystallite growth in graphitizing carbons and used a simple model to express changes in crystallite size as a function of temperature and heating time at maximum temperature. The specific resistivity of heat treated anthracite is closely related to the crystal lattice, and the model proposed by Richards can therefore be used to express the changes in electrical conductivity of anthracite by heat treatment.

The electrical conductivity, κ, in anthracite heat treated at a tempera-

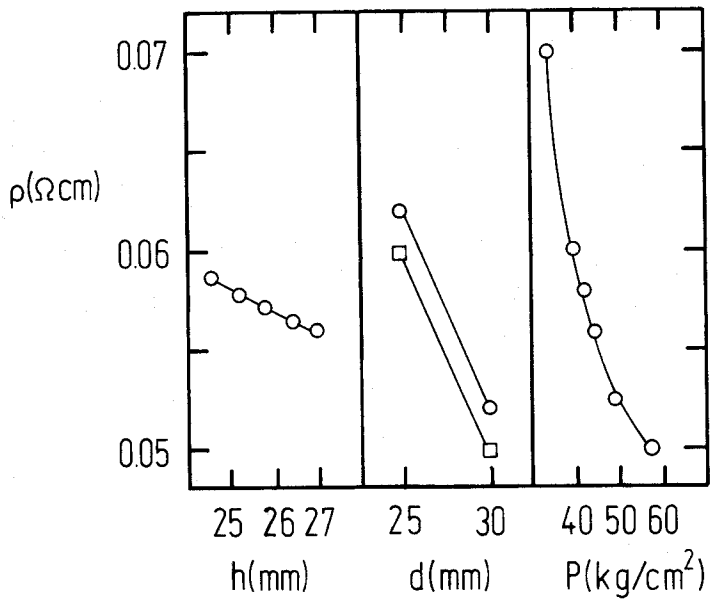

Figure 6. Correlation between electrical resistivity measured on powdered anthracite (20-65 mesh) and sample height, h; sample diameter, d, and pressure on the sample, P.

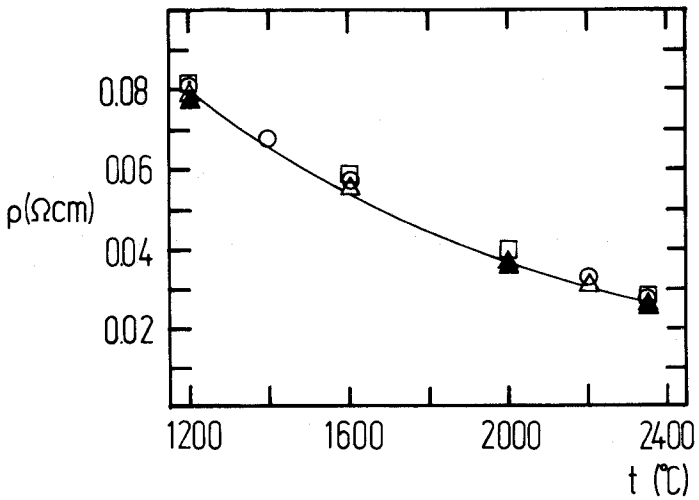

Figure 7. Electrical resistivity of anthracite *versus* heat treatment temperature at different heating rates and holding times. (□ - 400°C/h, 3h; o - 400°C/h, 4h; Δ - 400°C/h, 6h; ▲ - 200°C/h, 6h). The drawn line is calculated from the model described in the text [Eqn. (6)]. The holding time was 6 hours.

ture T,K for a holding time τ, can be represented by the empirical equation:

$$\kappa = a\tau^n \qquad (2)$$

where a and n are constants.

The suitability of this equation was confirmed by plotting the relevant isothermal data for different heat treatment temperatures, see Figure 8. The parallel straight lines demonstrates that Equation (2) can be used to describe the relationship between the electrical conductivity and the holding time. From linear regression analysis, n was calculated to be 0.087, with a standard deviation of 0.017. The fact that n is approximately independent of temperature suggests that in the temperature range from 1200°C to 2400°C, the activation energy for change in electrical conductivity does not have a spectrum of values, but can be described by a single value. At least this value will be a mean value for the activation energies in this region.

Richards found that a obeys the relation:

$$a = b \exp(-Q/RT) \qquad (3)$$

where b is a constant, Q is proportional to the activation energy, R is the gas constant and T is the heat treatment temperature in K.

Equations (2) and (3) can now be used to relate electrical conductivity, heat treatment temperature and holding time:

$$\kappa = b\tau^n \exp(-Q/RT) \qquad (4)$$

Studies of the change in crystallite height during heat treatment (15), show that the activation energy, E, is given by:

$$E = Q/n \; . \qquad (5)$$

In Equation (5), n is not a function of temperature as can be seen from Figure 8. If we assume that this relation also is valid for the change in electrical conductivity, the corresponding equation is obtained:

$$\kappa = b\tau^n \exp(-nE/RT) \; . \qquad (6)$$

A nonlinear parameter estimation data program (16) was used to evaluate the parameters in Equation (5) from the measured results of electrical conductivity, as shown in Table 1. The following parameter values were found:

$$b = 76 \text{ min}^{-1}$$

$$E = 340 \text{ kJ/mol}$$

$$n = 0.087 \; .$$

The absolute standard deviation of the fit was 0.048 and the relative standard deviation was 1.57%.

Compared to previous work (17,18), the calculated activation energy is about 50% lower than the values for the change in crystallite growth. Mitzushima (19) claimed that the activation energy for the change in electrical conductivity is identical to the activation energy for crystallite growth, and found that the activation energy rises from 314 kJ/mol to 878 kJ/mol in the temperature region from 1200 to 2400°C. However, these activation energies are apparent energies and can not be treated as absolute thermodynamic data.

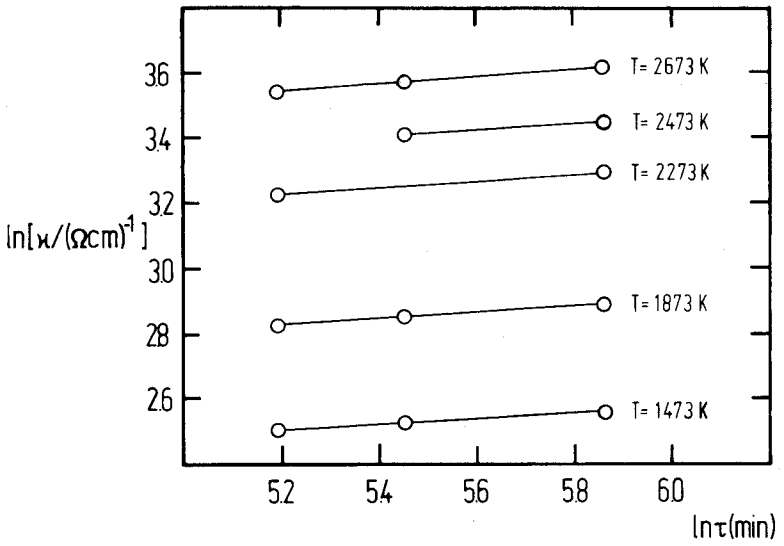

Figure 8. Logarithmic plot of electrical conductivity of anthracite *versus* holding time at different heat treatment temperatures.

Table 1. Electrical resistivity and conductivity of heat treated anthracite.

Temperature (K)	Holding time (min)	Resistivity (Ω cm)	Conductivity $(\Omega\ cm)^{-1}$
1473	180	0.082	12.2
1473	240	0.081	12.3
1473	360	0.079	12.7
1673	240	0.068	14.7
1873	180	0.059	17.0
1873	240	0.057	17.5
1873	360	0.056	17.9
2273	180	0.040	25.0
2273	360	0.037	27.0
2473	240	0.033	30.3
2473	360	0.032	31.3
2673	180	0.029	34.5
2673	240	0.028	35.7
2673	360	0.027	37.0

5. Industrial Calcining - Estimation of mean electrical conductivity

The electrical conductivity of calcined anthracite is an important quality parameter. Equation (6) gives the electrical conductivity as a function of the maximum temperature and the holding time at this temperature. This equation can then be used as basis for calculation of an average conductivity of the heat treated anthracite. Figure 9 shows a schematic cut through an electrical calciner. It is assumed that the volume between the electrodes has a constant temperature, T_e, and that the temperature falls off radially in a linear fashion. The following temperature functions result:

$$0 < r < r_e \qquad T = T_e \tag{7a}$$

$$r_e < r < r_w \qquad T = [T_e r_e - T_w r_w + r(T_e - T_w)]/(r_w - r_e) \tag{7b}$$

where

T - temperature at a radius r in the calciner (K)
T_e - temperature between the electrodes (K)
T_w - temperature at the wall of the calciner (K)
r_e - radius of the electrodes
r_w - inner radius of the calciner.

Combination of Eqns.(6) and (7) makes it possible to calculate the electrical conductivity of a material located at a distance r from the center. However, it is not trivial to calculate an average electrical conductivity of the material in the calciner, as the average conductivity depends on the particle size and how the materials are mixed. It is possible to calculate the two

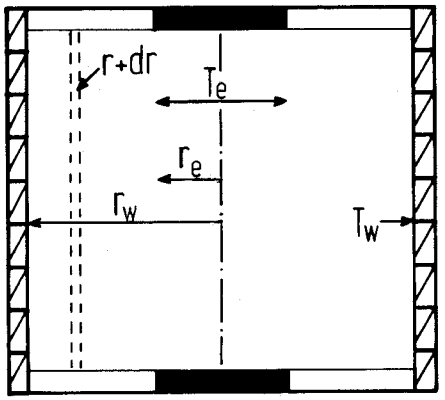

Figure 9. Schematic cut through an electrical calciner, where
T_e - temperature between the electrodes
T_w - temperature of the inner wall of the calciner
r_e - radius of the electrodes
r_w - inner radius of the calciner.

borderline cases . The maximum average conductivity is obtained when the mixed material can be considered as an array of parallel conductors, each array with the same conductivity. The average maximum conductivity is then obtained by integration of the electrical conductivities:

$$\bar{\kappa}_{max} = \frac{\kappa_e \cdot \pi r_e^2 + \int_{r_e}^{r_w} \kappa \cdot 2\pi r dr}{\pi r_w^2} \qquad (8)$$

where

κ_e - conductivity of the anthracite calcined between the electrodes
κ - conductivity of the anthracite calcined at a radius, $r_e < r < r_w$.

Similarly, the average minimum conductivity is obtained if the material with different conductivities can be assumed arrayed in a series. The integration has then to be carried out with respect to the resistivities:

$$\frac{1}{\bar{\kappa}_{min}} = \frac{\frac{1}{\kappa_e} \cdot \pi r_e^2 + \int_{r_e}^{r_w} \frac{1}{\kappa} \cdot 2\pi r dr}{\pi r_w^2} \qquad (9)$$

The integrals are solved numerically by insertion of Eqns.(6) and (7) and the results for some typical cases are presented in Fig. 10. A reasonable assumption is to give the average conductivity $\bar{\kappa}_{av}$ as the mean of $\bar{\kappa}_{max}$ and $\bar{\kappa}_{min}$, as shown by heavy drawn lines in Fig. 10. The figure represents a model for the anthracite showing how the electrical conductivity depends on T_e, T_w and the holding time. From Figure 10 it is for instance seen that a doubling of the holding time from 3 to 6 hours is equivalent to an increase of T_e with 200°C. Similarly it is seen that a 200°C increase of the wall temperature increases the conductivity more than a 200°C increase of the temperature between the electrodes. This is then an argument for proper wall insulation of the calciner.

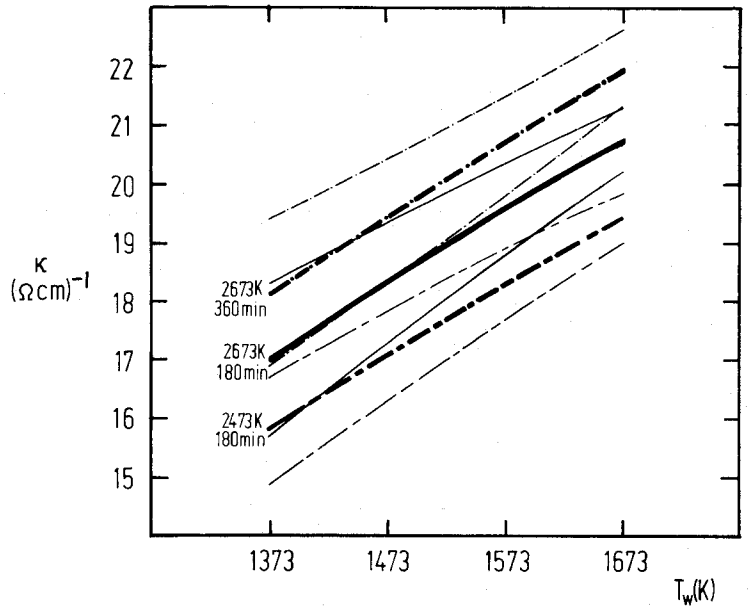

Figure 10. Electrical conductivity of calcined anthracite calculated from the model described in the text at different temperatures at the inner wall of the calciner and different temperatures between the electrodes and when the average holding time are varied. The heavy drawn lines is the average between the values calculated from Eqn. (8) and Eqn. (9),which are drawn with thin lines.

Acknowledgement. Thanks are due to Professor K. Motzfeldt for experimental advice and to Dr.ing. T. Foosnæs and Dr.ing. T. Naterstad for helpful criticism.

References

1. Williams, M.M., "Electrically Calcined Anthracite for Potlinings", presented paper at AIME Meeting, San Fransisco Feb. 1972, Light Metals 1972.
2. Belitskus, D., "Effect of Anthracite Calcination and Formulation Variables on Properties of Bench Scale Aluminium Smelting Cell", Met. Trans. 8B (1977) 591.
3. Ritter, H.L. and Drake, L.C., "Pore Size Distribution in Porous Materials", Ind. Eng. Chem. Anal. ed. 17, (1945) 782.
4. Neher, M.B., "Extended Range Hydraulic Mercury Porosimeter", Anal. Chem. 33, no. 8 (1961) 1132.
5. Ergun, S., "X-ray Studies of Carbon"in Chemistry and Physics of Carbon, P.L. Walker ed., Vol. 3, Marcel Dekker Inc., New York 1968.
6. Fushizaki, Y., Youshimura, F. and Mitsui, S., in Japanese, Kogyo Kagaku Zasshi (Japan) 65 (1965) 81.
7. Kelly, B.I., "Physics of Graphite", Applied Science Publishers 10, London 1982.
8. Miura, S. and Silveston, P.L., "Change of Pore Properties During Carbonisation of Coking Coal", Carbon 18 (1980) 93.
9. Wallouch , R.W. and Fair, F.V., "Kinetics of the Shrinkage Prosess during Calcination", Carbon 18 (1980) 147.
10. Fitzer, E., "Evidence of Catalytic Effect of Sulphur on Graphitization between 1400 and 2000°C", Carbon 14 (1976) 195.
11. Whittaker, M.P. and Grindstaff, L.I., "The Irreversible Expansion of Carbon Bodies During Graphitization", Carbon 7 (1969) 615.
12. Maire, J. and Mering, J., "Graphitization of Soft Carbons"in Chemistry and Physics of Carbon, P.L. Walker ed., Vol. 6, Marcel Dekker Inc., New York 1970.
13. Evans, El. L., Jenkins, J.L. and Thomas, J.M., "Direct Electron Microscopic Studies of Graphitic Regions in Heat Treated Coals and Coal Extracts", Carbon 10 (1972) 637.
14. Richards, B.P., "Activation Energies for Crystallite Growth and Ordering in Graphitizing Carbons", Journal of Crystallite Growth 34 (1976) 325.
15. Murty, H.N., Biedermann, D.L. and Heinz, E.A., "Kinetics of Graphitization. II. Pre-Exponential Factors", Carbon 7 (1969) 683.

16. Hertzberg, T., MODFIT, Chem. Eng. Lab., Norwegian Institute of Technology, Trondheim 1982.

17. Pacault, S., "The Kinetics of Graphitization", in Chemistry and Physics of Carbon , P.L. Walker ed., Vol. 7, Marcel Dekker Inc., New York 1971.

18. Fischbach, P., "The Kinetics and Mechanism of Graphitization" in Chemistry and Physics of Carbon , P.L. Walker ed., Vol. 7, Marcel Dekker Inc., New York 1971.

19. Mitsushima, S., "Rate of Graphitization of Carbon", Proc. 5th Carbon Conf., Pergamon Press, New York 1963.